ADVANCED FUNCTIONAL MATERIALS

Supporting Information

for *Adv. Funct. Mater.*, DOI: 10.1002/adfm.201804456

Weaving Sensing Fibers into Electrochemical Fabric for Real-Time Health Monitoring

*Lie Wang, Liyuan Wang, Ye Zhang, Jian Pan, Shangyu Li, Xuemei Sun, Bo Zhang, and Huisheng Peng**

Supporting information

Figure S1. Photograph of a roll of CNT fiber.

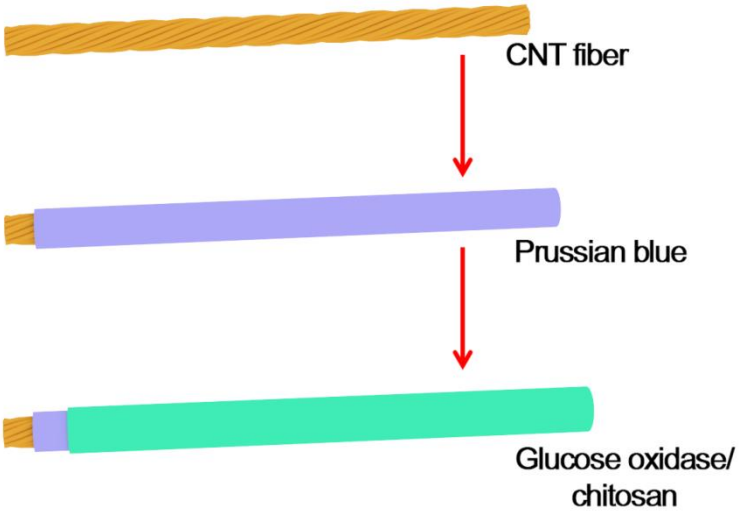

Figure S2. Schematic illustration for the fabrication of glucose-sensing fiber.

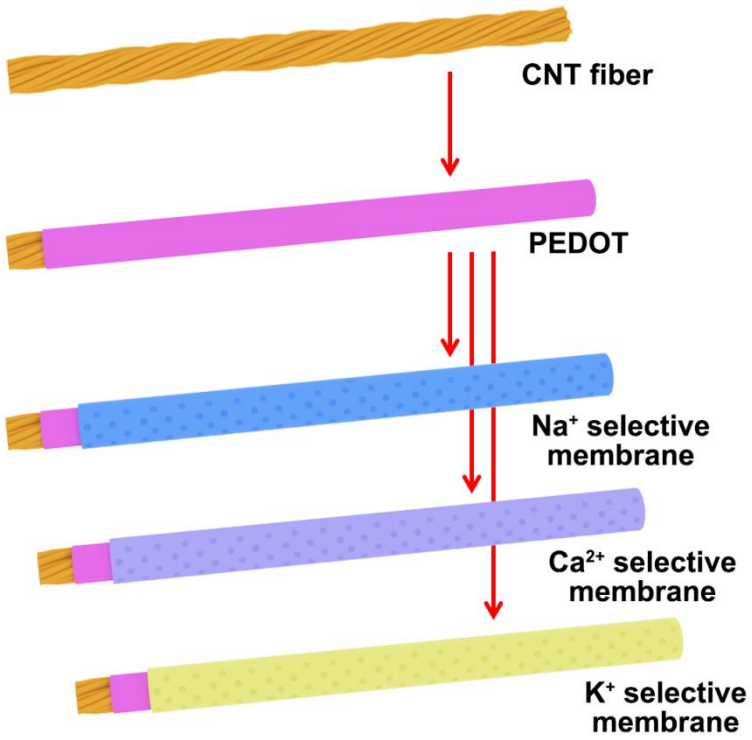

Figure S3. Schematic illustration for the fabrication of Na^+, Ca^{2+} and K^+-sensing fibers.

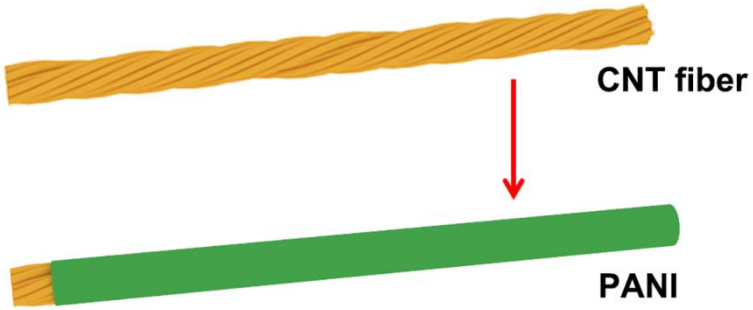

Figure S4. Schematic illustration for the fabrication of pH-sensing fiber.

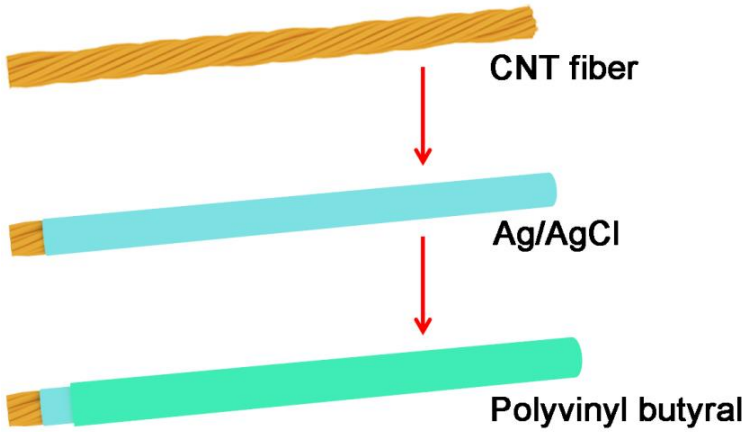

Figure S5. Schematic illustration for the fabrication of Ag/AgCl reference fiber.

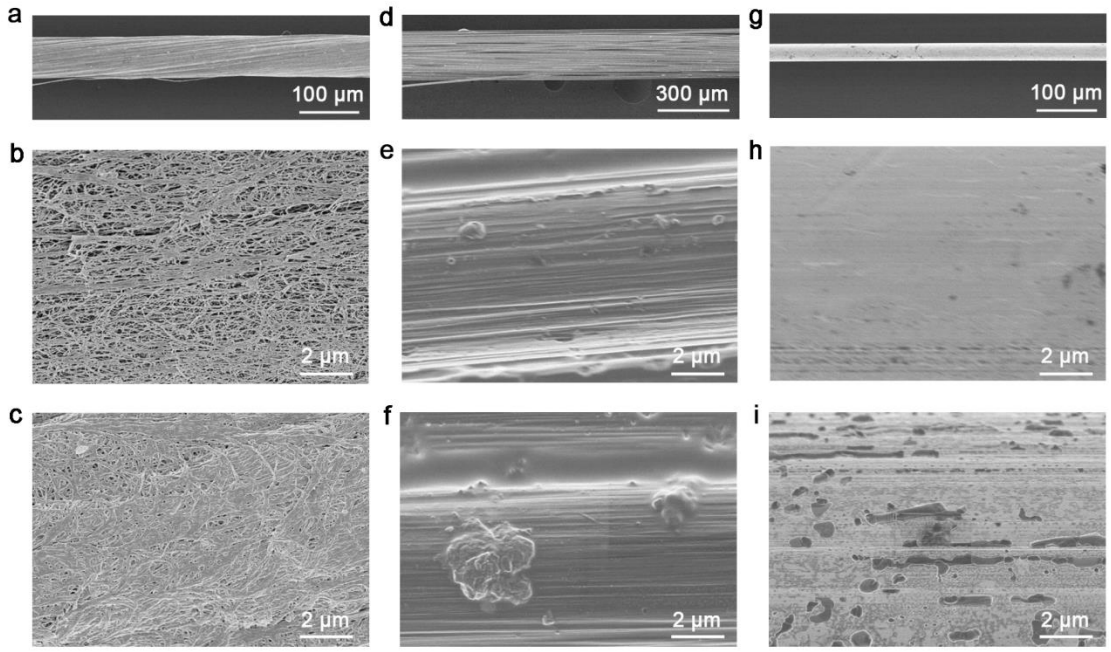

Figure S6. SEM images of the CNT fiber at **a)** low, **b)** high magnifications and **c)** after electrodeposition of PANI. SEM images of the carbon fiber at **d)** low, **e)** high magnifications and **f)** after electrochemical deposition of PANI. SEM images of the Au wire at **g)** low **h)** high magnifications and **i)** after electrodeposition of PANI.

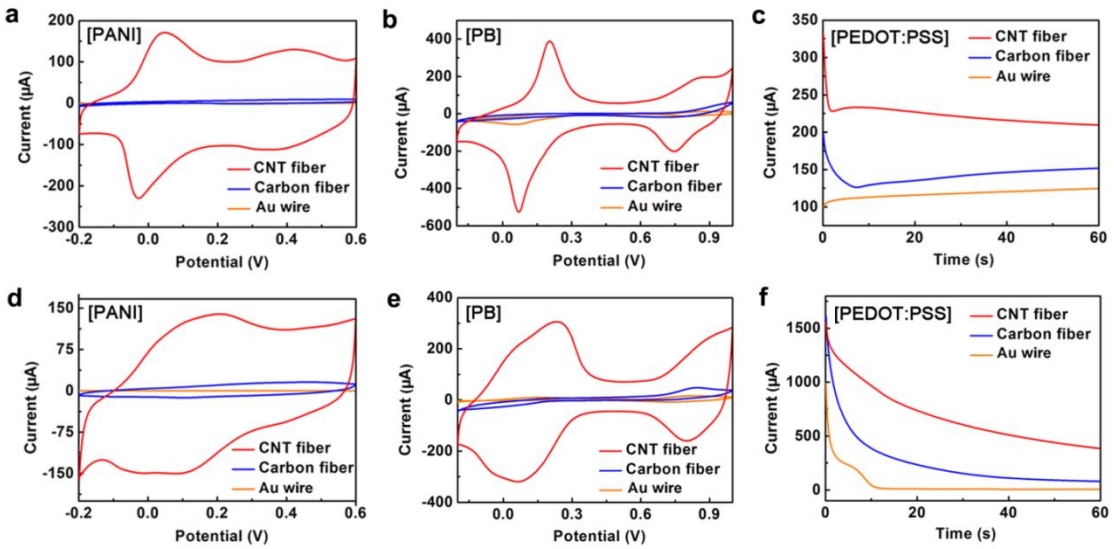

Figure S7. a) and **b**) CV plots of the electrodes during the PANI and PB electrodeposition process (scan rate of 100 $mV \cdot s^{-1}$ with a commercial saturated calomel electrode). **c)** Amperometric curves of the electrodes during the PEDOT electrodeposition process (initial potential of 1.25 V versus a commercial Ag/AgCl electrode). **d**) and **e**) CV plots of the electrodes in PBS after electrodeposition of PANI and PB (scan rate of 100 $mV \cdot s^{-1}$ with a commercial Ag/AgCl electrode). **f)** Amperometric curves of the electrodes in PBS after electrodeposition of PEDOT:PSS (initial potential of 1.25 V versus a commercial Ag/AgCl electrode).

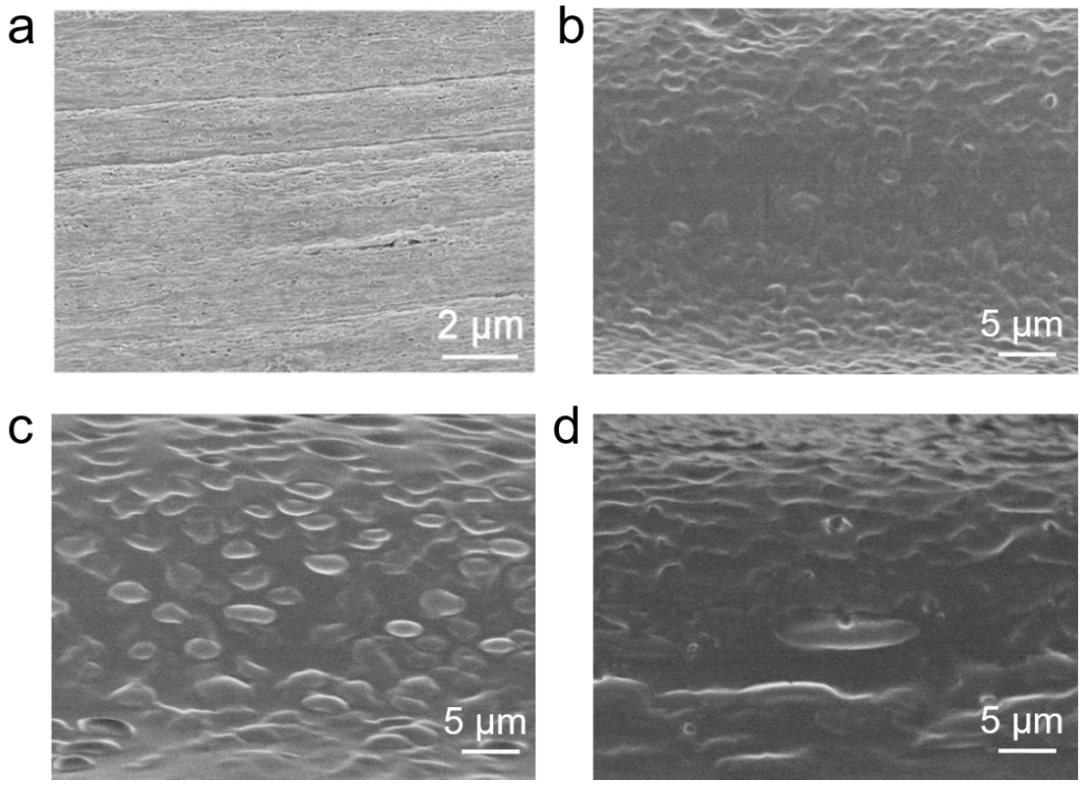

Figure S8. SEM images of the Na^+, K^+ and Ca^{2+}-sensing fibers. **a)** PEDOT:PSS layer. **b)** Na^+-selective membrane layer of Na^+-sensing fiber. **c)** K^+-selective membrane layer of K^+-sensing fiber. **d)** Ca^{2+}-selective membrane layer of Ca^{2+}-sensing fiber.

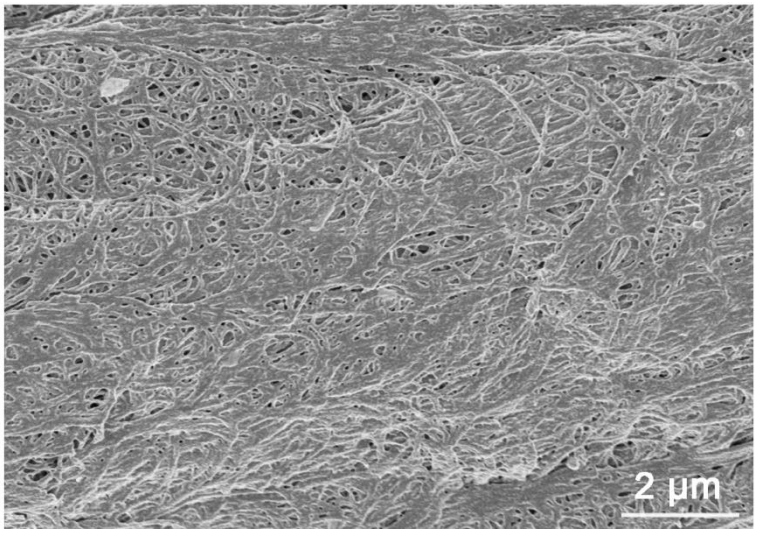

Figure S9. SEM image of the PANI layer of the pH-sensing fiber.

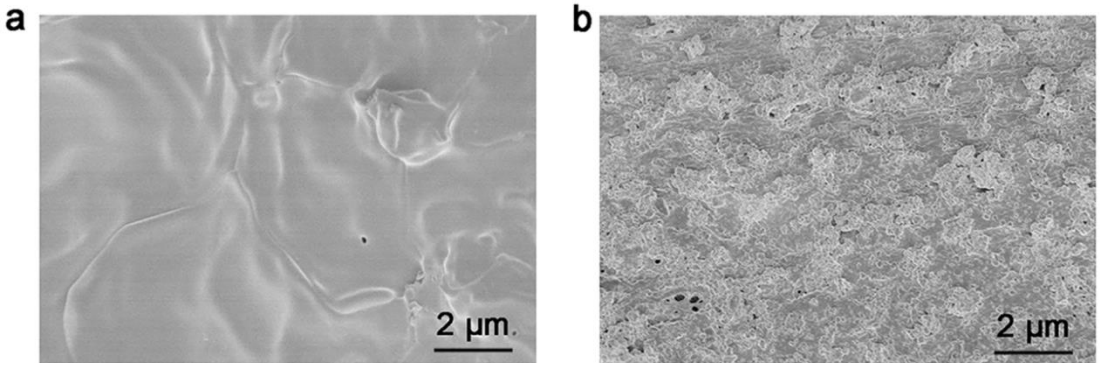

Figure S10. SEM images of the Ag/AgCl fiber electrode. **a)** Ag/AgCl layer. **b)** PVB layer.

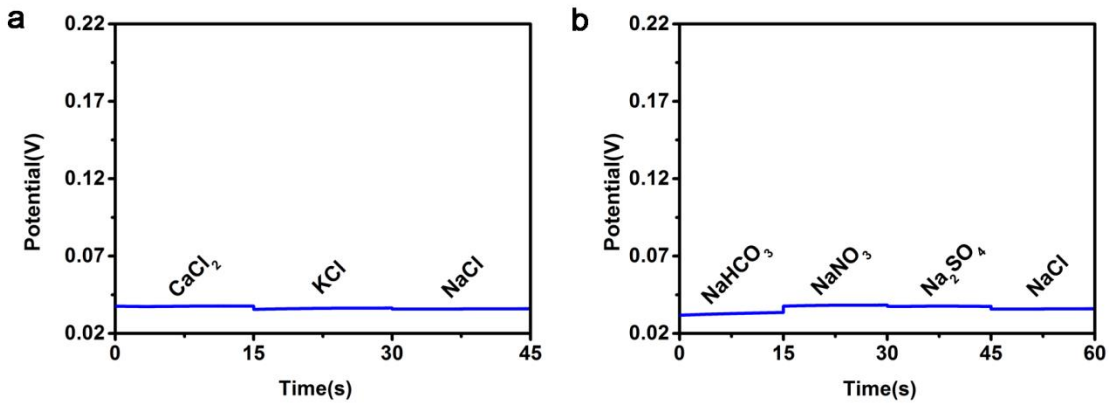

Figure S11. The stability of a Ag/AgCl fiber electrode in solutions containing 50 mM NaCl and 10 mM of different **a)** cationic and **b)** anionic solutions.

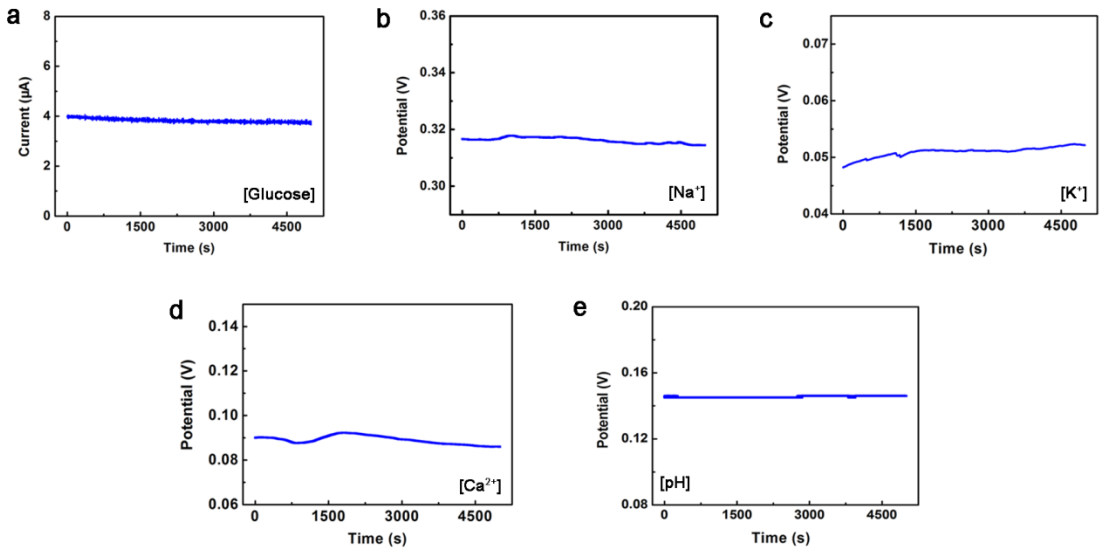

Figure S12. The long-term stability of the **a)** glucose, **b)** Na^+, **c)** K^+, **d)** Ca^{2+}, and **e)** pH-sensing fibers.

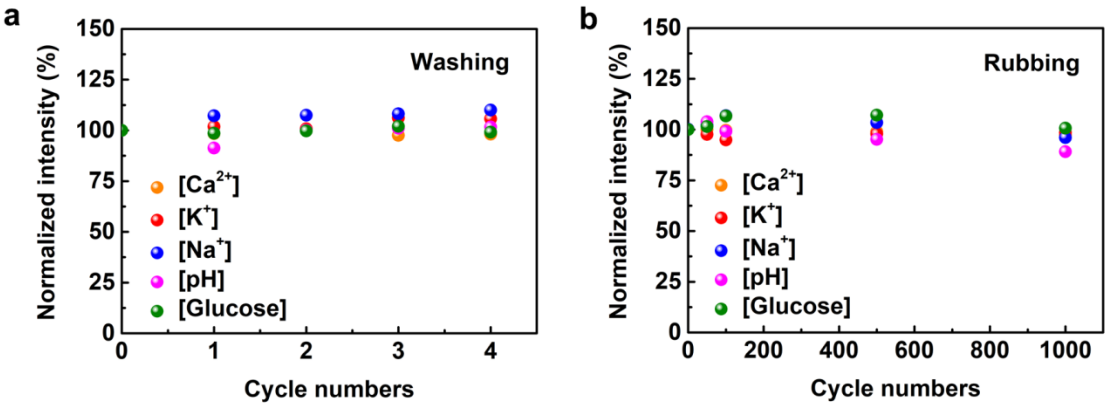

Figure S13. a) Washability and **b)** rubbing resistance of the sensing fibers in electrochemical fabric under repeated water washing and rubbing.

Figure S14. Photograph of a garment device embedded with sensing fiber units knitted into the fabric.

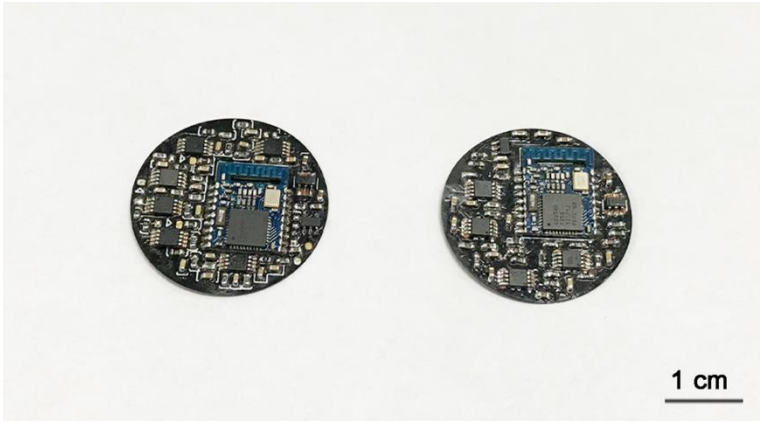

Figure S15. Photograph of two flexible integrated chips.

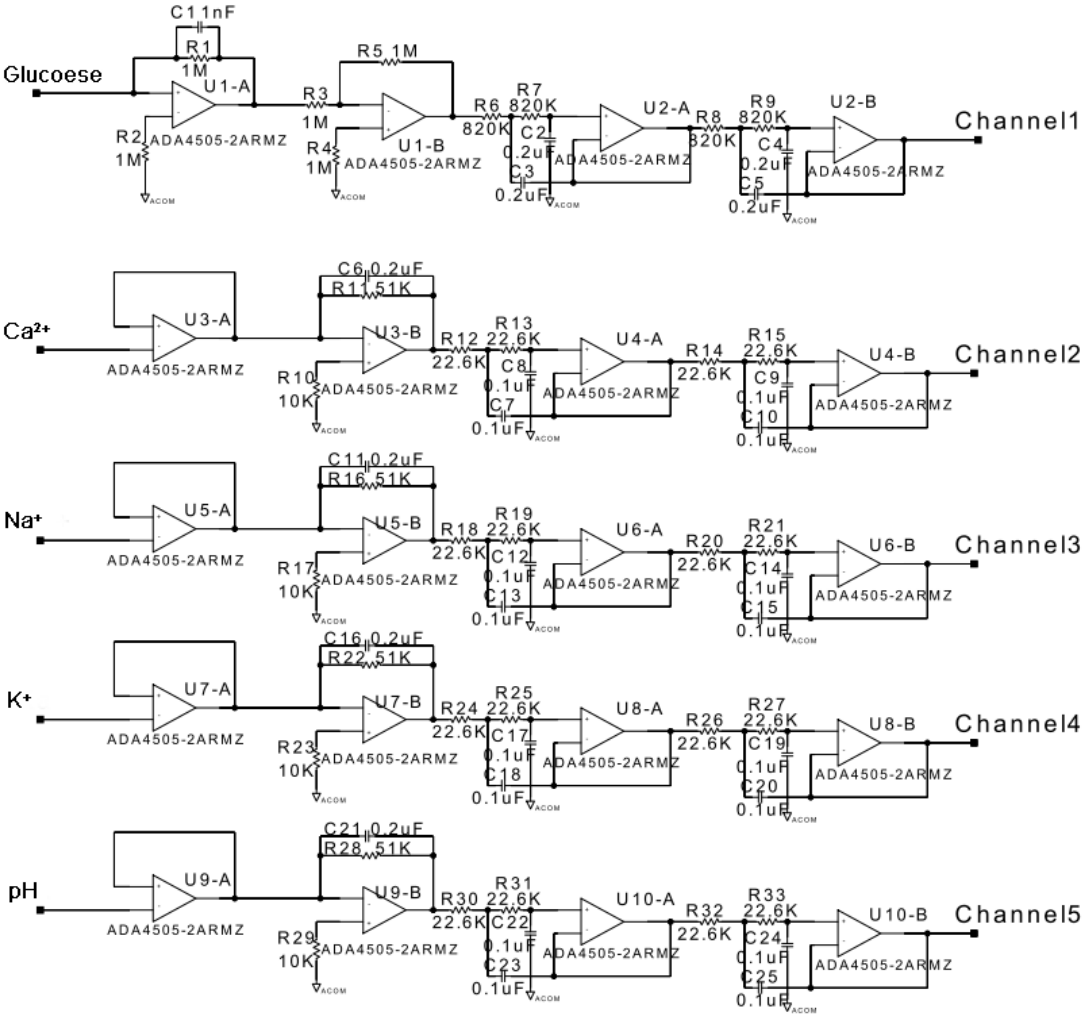

Figure S16. Schematic diagram for the signal-conditioning circuit.

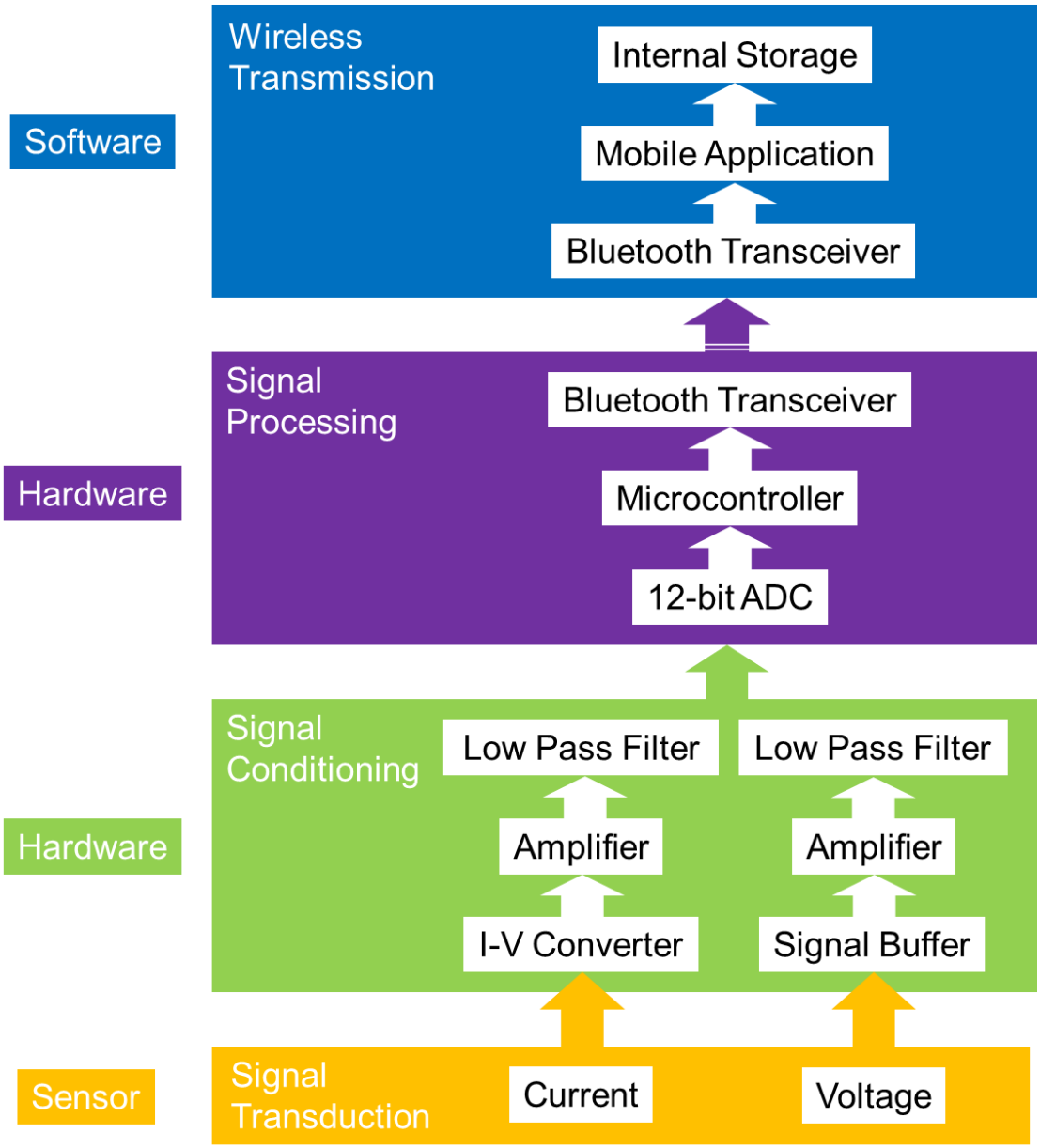

Figure S17. System-level block diagram of the wearable electrochemical fabric platform.

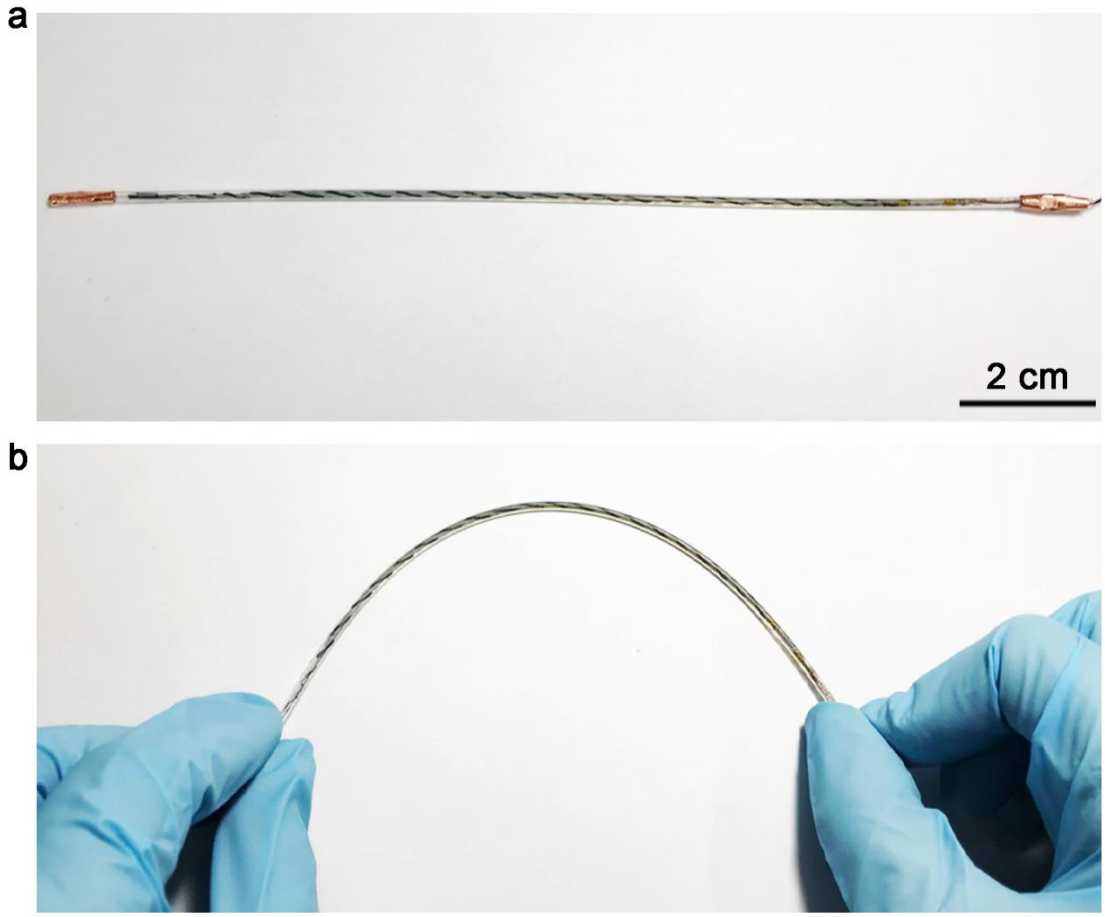

Figure S18. Photographs of a flexible, fiber-shaped, lithium ion battery.